

## X-ray diffraction studies of the structure of nanometer-sized crystalline materials

X. Zhu, R. Birringer, U. Herr, and H. Gleiter

*Werkstoffwissenschaften, Universitaet des Saarlandes, D-6600 Saarbruecken, West Germany*

(Received 8 July 1986; revised manuscript received 3 December 1986)

Recently, nanometer-sized crystalline materials have been proposed to represent a new solid-state structure which exhibits neither long-range order (like crystals) nor short-range order (like glasses). It was the purpose of this study to test this idea by x-ray diffraction experiments. Nanometer-sized crystalline materials are polycrystals in which the size of the crystallites is a few (1–10) nanometers. Structurally, these materials consist of the following two components, the volume fraction of which is about 50% each: a crystalline component, formed by all atoms located in the lattice of the crystallites, and an interfacial component comprising the atoms situated in the interfaces. It is this interfacial component which was proposed to exhibit an atomic arrangement without short- or long-range order. In order to test this idea, the interference function of nanometer-sized crystalline iron (6-nm crystal size) was measured by x-ray diffraction. The measured interference function was compared with the interference function computed by assuming the interfacial component to be short-range ordered or to consist of randomly displaced atoms (no short- or long-range order). It was found that the experimental interference function can only be matched by the computed one if the interfacial component is assumed to have no short- or long-range order.

### I. INTRODUCTION

All solids may be classified structurally into two categories: crystalline materials with long-range order or glasses with short-range order [Figs. 1(a) and 1(b)]. As many properties of solids depend primarily on the nearest-neighbor configurations, e.g., interatomic potentials or the exchange energy of three-dimensional ferromagnets, it seems attractive to develop a new category of solid materials which differ from glasses and crystals in the sense that they exhibit little short-range or long-range order [Fig. 1(c)]. This new type of solid-state structure has been suggested recently to exist in nanometer-sized crystalline materials<sup>1</sup> for the following reasons.

Nanometer-sized crystalline materials are polycrystals in which the size of individual crystallites is on the order of several (1–10) nanometers (Fig. 2). These materials consist of the following two components: A crystalline component formed by all atoms located in the lattice of the crystallites (grains) and an interfacial component comprising all atoms which are situated in the grain (or interphase) boundaries between the crystallites. The atomic structure of an interface is known<sup>2</sup> to depend on the orientation relationship between adjacent crystals and the boundary inclination. If the crystallites are oriented at random, all of the grain boundaries of a nanometer-sized crystalline material have different atomic structures characterized by, e.g., different interatomic spacings. In Fig. 2, for example, the different interatomic spacings are indicated by arrows in the boundaries *A* and *B*. A nanometer-sized crystalline material with a crystallite size of 5 nm contains typically about  $10^{19}$  interfaces per  $\text{cm}^3$ . The interfacial component is the sum of the  $10^{19}$  interfacial structures. If the interatomic spacings in all boundaries are different, the average of  $10^{19}$  different boundaries results in no preferred interatomic spacings except

for the one prevented by interatomic penetration [Fig. 1(c)]. Hence, the interfacial component is proposed to represent the solid-state structure without long- or short-range order.

The purpose of this investigation is to study the structure of the interfacial component by comparing the interference function deduced from the x-ray diffraction experiments with the one calculated from different structural models of nanometer-sized crystalline materials.

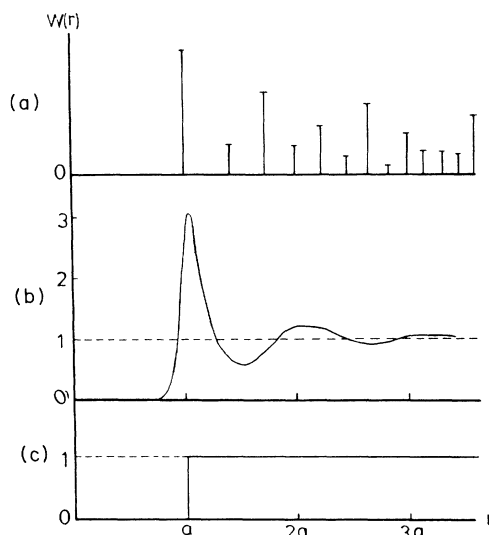


FIG. 1. The probability functions  $W(r)$  for interatomic distances of a one-element system which express the probability that the centers of two specified atoms should lie at a distance  $r$  apart. (a) Long-range-ordered crystalline structure; (b) short-range-ordered glassy structure; (c) neither long- nor short-range-ordered structure.

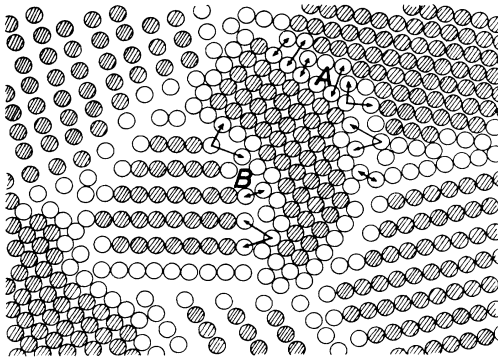


FIG. 2. Schematic cross section through a nanometer-sized crystalline material (hard-sphere model). The different interatomic spacings in the grain boundaries *A* and *B* are indicated by arrows. In reality, the atoms are known to relax from the ideal lattice sites given by a hard-sphere model. The relaxation involves the atoms at the boundary and extends several layers into the lattice of the adjacent crystals (Ref. 2).

## II. EXPERIMENTAL PROCEDURE

Nanometer-sized crystalline  $\alpha$ -Fe samples (thickness  $\sim 15 \mu\text{m}$ , diameter  $\sim 5 \text{mm}$ ) were prepared by compacting small iron crystals into a solid. The small crystals were produced by an inert gas condensation technique.<sup>3</sup> The average crystallite size measured by means of transmission electron microscopy (TEM) was about 6 nm. The mass density of the samples was  $6.5 \text{g/cm}^3$ , i.e., 83% of the bulk density. The density was determined by means of measurements of the volume and the mass of the sample. The samples were studied by means of x-ray diffractometer in transmission mode. The scattered intensity versus scattering angle ( $2\theta$ ) was measured using molybdenum radiation, a quartz diffracted beam monochromator, and a scintillation counter in connection with a discriminator. The interference function per atom  $I(s)$  ( $s$  is the magnitude of the wave vector,  $s = 2 \sin\theta/\lambda$ ) was deduced from the measured intensity by the following procedure.

The measured intensity was corrected for polarization, absorption, and inelastic scattering and normalized to electron units per atom to deduce the coherent scattering  $I_c(s)$  according to Ref. 4. The interference function per atom,  $I(s)$ , was obtained in absolute units from  $I(s) = I_c(s)/f^2$ , where the complex form of the atomic scattering factor  $f$  was used in order to account for anomalous scattering.<sup>5</sup> The impurity concentration of the specimen measured by means of mass spectroscopy, electron spectroscopy for chemical analysis (ESCA), and atomic absorption analysis was 0.5 wt. % or less.

## III. COMPUTATION OF THE X-RAY SCATTERING OF NANOMETER-SIZED CRYSTALLINE MATERIALS

Due to the small size of the crystallites of a nanometer-sized crystalline material, the numbers of

atoms located in the crystalline component and in the interfacial component are comparable. Hence, the computation of the x-ray scattering of a nanometer-sized crystalline material requires the computation of the scattering due to the differently oriented crystals as well as the computation of the scattering originating from the interfacial regions. The existence of x-ray scattering from interfacial regions and its usefulness to obtain information about the atomic structure of interfaces has been demonstrated by Sass *et al.*<sup>6</sup> The physical reason for the scattering from the interfacial regions is the interference between the x rays scattered by the atoms forming the interfaces, e.g., the scattering due to atoms marked by arrows in Fig. 2.

It has been shown<sup>7</sup> that the scattering of the differently oriented crystals of a polycrystal material with a random texture may be computed by means of the following procedure. A single crystal the size of which is equal to the average crystal size of the polycrystalline material is considered. This crystal represents the ensemble average of the individual crystallites of the polycrystal. For this crystal the interference function  $I(s)$  for a specific orientation of the crystal with respect to the incident x ray is computed. This procedure is repeated for all possible orientations of the crystal and the resulting functions  $I(s)$  are averaged for  $s = \text{const}$ . If the averaging procedure is repeated for all possible values of  $s$ , the resulting function  $I(s)$  has been shown to be the interference function of the polycrystal with a random texture. By following the same procedure, the scattering from the crystalline and interfacial components of nanometer-sized crystalline material was computed.

In fact, for the specific case of the nanometer-sized crystalline iron studied, the crystalline component was modeled by a cube-shaped  $\alpha$ -Fe-(bcc) crystal representing the ensemble average of the crystalline component. The volume of this cube was matched to the average volume of the crystallites of the nanometer-sized crystalline Fe measured by transmission electron microscopy. The ensemble average of the interfacial component was simulated by an assemblage of atoms whose structure can be varied between the two known extremes: a crystalline structure and a structure without any short-range order [Figs. 1(a) and 1(c)]. These two extremes were chosen because the atomic structures of the boundaries and hence their ensemble average are not known exactly. A variation of the ensemble average between crystalline order and no short-range order covers all conceivable boundary structures. The interfacial component consisted of an assemblage of atoms arranged in the form of two layers of atoms with  $\alpha$ -Fe structure attached coherently at the outer surface of the cube. Subsequently, the atoms in the two outer layers were displaced by nonlattice vectors in randomly chosen directions. A variation of the number of layers was used to simulate boundaries of different widths. The effects of crystallite size and crystallite size distributions were accounted for by adjusting the size of the cube to the measured values of the crystallite size and by using the experimental data obtained by TEM. By varying the magnitude of the random atomic displacements in the outer layers, interfacial components varying between the two extremes mentioned were simulated. The

thermal diffuse scattering of the crystalline component at room temperature was simulated by randomly displacing the crystal atoms by 3% of the nearest-neighbor distance (NND) which corresponds to the attenuation of the diffraction peaks of  $\alpha$ -Fe at room temperature.

The interference function  $I(s)$  of the crystalline and the interfacial component was computed from the following equation:

$$I(s) = \frac{1}{N} \left| \sum_{j=1}^N \exp[2\pi i(\mathbf{r}_j \cdot \mathbf{s})] \right|^2, \quad (1)$$

where  $N$  is the total number of atoms in the system,  $\mathbf{s}$  is the scattering vector, and  $\mathbf{r}_j$  characterizes the coordinates of the atom  $j$ . The computed three-dimensional function  $I(s)$  was reduced to a one-dimensional plot  $I(s)$  by following the averaging procedure for  $I(s)$  described in the previous paragraph. In the vicinity of the Bragg maxima, the interval  $\Delta s$  between neighboring  $s$  values was 0.0061. In the region between the peaks,  $\Delta s$  was 0.0175. The  $s$  was varied between  $s=0.1$  and  $1.7$ .<sup>8</sup> The one-dimensional plot  $I(s)$  was compared with the experimental interference function  $I(s)$ . All computed interference functions were convoluted by a Gaussian instrument function in order to simulate the effect of instrumental broadening of the diffractometer used for the experiments.

The effect of interparticle interference is not included in  $I(s)$ . However, interparticle interference has been shown to yield only nonvanishing scattering in the small-angle region<sup>9</sup> which is not within the scope of this paper.

#### IV. RESULTS AND DISCUSSION

The experimentally measured interference function of nanometer-sized crystalline Fe is shown in Fig. 3. The number of peaks and their positions are consistent with the reflections of bulk bcc  $\alpha$ -Fe. The observed interference function is characterized by the following features: a diminishing peak-to-background ratio as the scattering vector increases, and a growing background intensity starting at  $s=0.15$  and approaching unity at  $s=1.4$ .

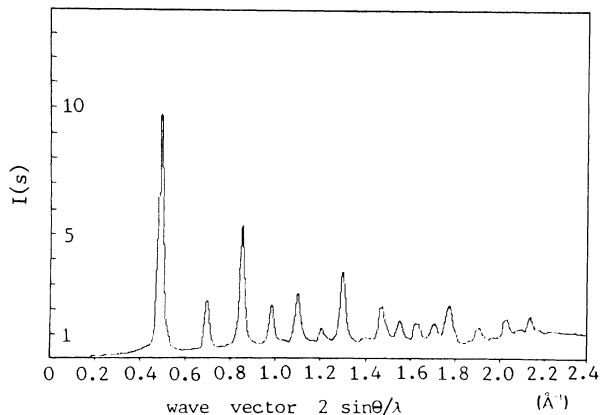


FIG. 3. The measured interference function per atom for nanometer-sized crystalline Fe (6 nm).

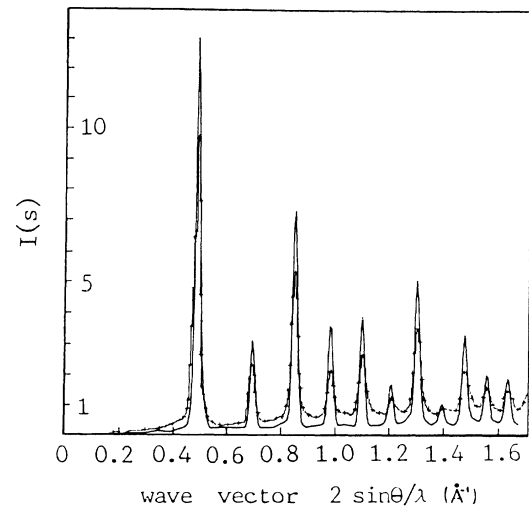


FIG. 4. Comparison of the measured (--- +--) and computed (—) interference functions for nanometer-sized crystalline Fe. The model system assumed for the computations is a boundary structure consisting of four atomic layers in which atoms are randomly displaced. The displacements of the atoms corresponding to the two layers in the boundary core are assumed to be 15% of the NND, in the two adjacent layers the displacements are 7% of the NND. The displacement of 15% of the NND corresponds to the average nearest-neighbor displacement of the atoms in a  $\text{Fe}_{80}\text{B}_{20}$  glass (Ref. 10).

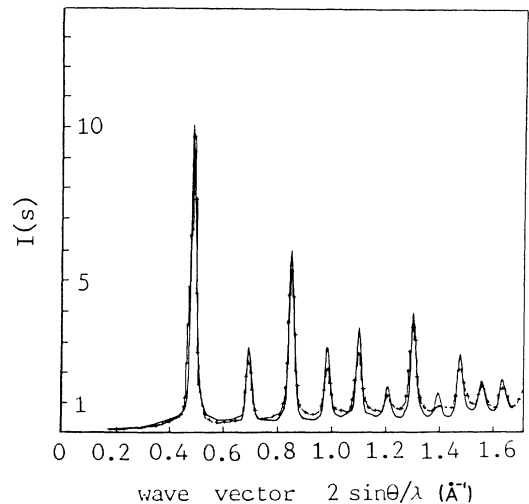


FIG. 5. Comparison of the measured and computed interference functions of nanometer-sized crystalline Fe. The model system assumed for the computations is a boundary structure consisting of four atomic layers in which atoms are randomly displaced. The displacements of the atoms corresponding to the two layers in the boundary core are assumed to be 50% of the NND, in the two adjacent layers the displacements are 25% of the NND.

A comparison of the experimental and the computed interference functions is shown in Fig. 4 assuming a short-range-ordered grain boundary structure. The boundaries were assumed to have a thickness of four atomic layers, which agrees with the present knowledge of the atomic structure of grain boundaries in metal.<sup>2</sup>

Although the peak positions and the widths of the computed  $I(s)$  are consistent with the experimental observation, the calculated peak heights are exceeded and the calculated attenuation is slower than the experimentally observed one. Furthermore, the calculated background is too low in the range between  $s=0.1$  and  $0.45$  (below the position of the first peak). The discrepancy increases at large  $s$ . The poor agreement between the computation and experiment suggests that the model based on a short-range-ordered grain boundary component cannot satisfactorily explain the experimental observation.

In a second set of computations, an attempt was made to match the experimental data by assuming a non-short-range-ordered grain boundary component. A structure of this type was generated by displacing the boundary atoms as described in the caption of Fig. 5. It may be seen that the computed  $I(s)$  curve reproduces not only the heights and widths of all the peaks, but also matches approximately the background intensity, especially in the regime between  $s=0.1$  and  $0.45$  where the fit with the model assuming a short-range-ordered interfacial component (Fig. 4) was particularly poor. It may be mentioned here that the growing background intensity in this regime in Fig. 3 is consistent with the observation of Sass *et al.*<sup>6</sup> Nevertheless, some discrepancy between the computed and observed  $I(s)$  curves remains at large values of  $s$ . In fact, this discrepancy is reduced further by taking the size distribution of the crystallites into account. Figure 6 shows the agreement between theoretical and experimental

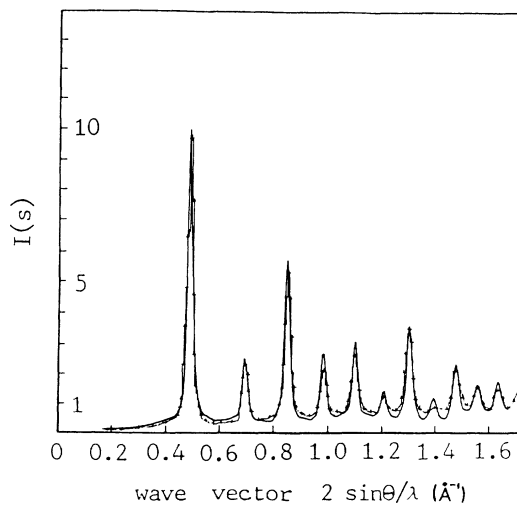


FIG. 6. Comparison of the measured and computed interference functions of nanometer-sized crystalline. The model computed is a mixture of 6-nm (75 vol. %) and 4-nm (25 vol. %) crystals in which the boundary atoms are randomly displaced in the same way as in the case of Fig. 5.

data, if the nanometer-sized crystalline Fe is assumed to consist of 75 vol. % of 6-nm crystallites and 25 vol. % of 4-nm crystallites; the size distribution assumed was based on TEM observations.<sup>11</sup>

The computer simulations failed to reproduce the experimental  $I(s)$  for the models of multilayered boundary component (eight layers), smaller crystallite size (4 nm), and large atomic displacements (60% of the NND in the first outer layer and 30% of the NND in the second outer layer of the one-crystal system).

Furthermore, it was not possible to reproduce the experimental data with an enhanced thermal diffuse scattering by assuming a model of an assemblage of small crys-

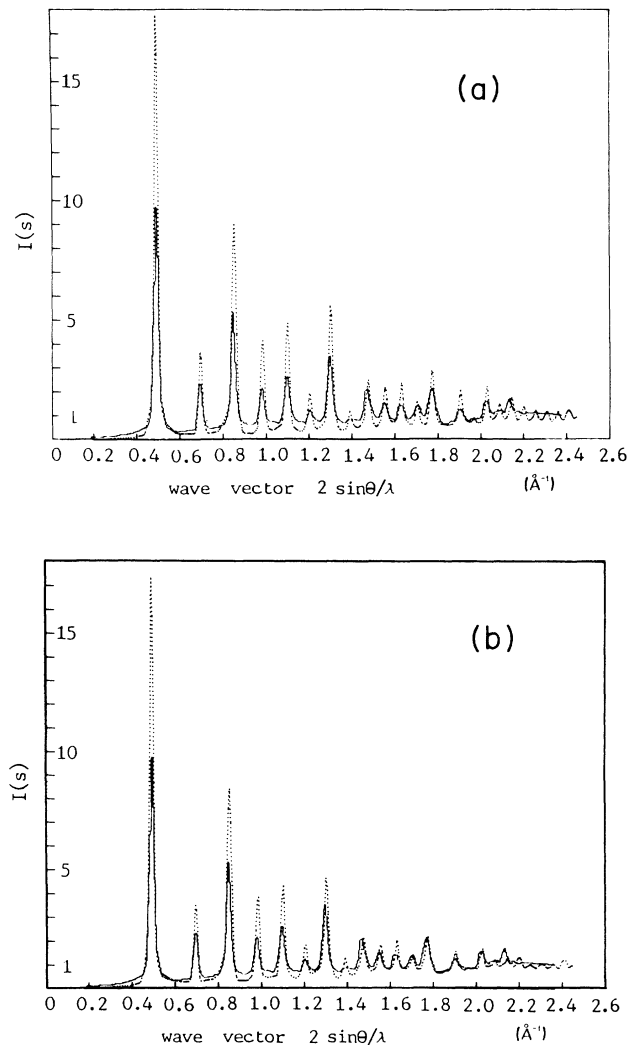


FIG. 7. Comparison of the measured (—)  $I(s)$  of nanometer-sized crystalline Fe and the computed interference functions of isolated 6-nm Fe crystallites with enhanced thermal diffuse scattering. All atoms in the model were randomly displaced with a parameter of (a) 5% of the NND ( $\cdot \cdot \cdot$ ) or (b) 6% of the ND ( $\cdot \cdot \cdot$ ). No grain-boundary structure was included in the computation.

tallites that are not connected by grain boundaries. Figure 7 shows the comparison between the experimental and the computed  $I(s)$  curves for 6-nm crystallites in which all atoms were randomly displaced by 5% and 6% of NND, respectively. At  $s=1.85$ , where the  $h^2+k^2+l^2=28$  reflection is missing, the computed intensities match [5% of NND, Fig. 7(a)] or exceed [6% of NND, Fig. 7(b)] that of the experimental. However, in the range between  $s=0.1$  and 0.45, none of the computed curves can reproduce the experimental data. This discrepancy results from neglecting grain-boundary scattering and does not seem to originate from the accuracy of the computations.

In fact, the agreement between the experimental and computed  $I(s)$  curves may be seen for 6-nm Au crystals which are isolated from one another so that no grain boundaries can be formed (Fig. 8). In the computation, the lattice parameter of gold and a displacement parameter of 5% of NND were used. The latter matches the amplitude of thermal vibration of 6-nm gold crystallites reported in Ref. 13.

In the previous iron computations, a constant mass density corresponding to the bulk crystalline density was used. It cannot explain the density deficit observed in the experiments. Furthermore, if the atoms in the first outer layer are displaced by 50% of the NND (Fig. 5), some atoms overlapped. In order to match the computations to the experimentally measured density of the nanometer-sized crystalline Fe specimens, the density variation was assumed to originate totally from a density deficit in the grain boundaries. A lower density of the interfacial component was simulated for the conditions given in Fig. 5 by scaling the interatomic distances in the outer (displaced) layers according to the experimental density data. The re-

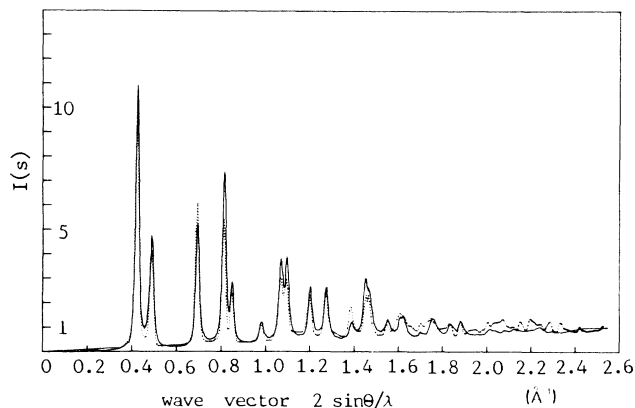


FIG. 8. Comparison of the measured (—) and computed (· · ·) interference functions of isolated Au crystallites. The correction procedure of the measured data was the same as that for Fe. The average size of Au crystallites obtained by means of Fourier transform of the measured  $I(s)$  is 6 nm. In the model system, an overall displacement parameter of 5% of the NND of Au was used which matches the amplitude of the thermal vibration of 6-nm Au crystallites in Ref. 13. No grain-boundary structure was considered.

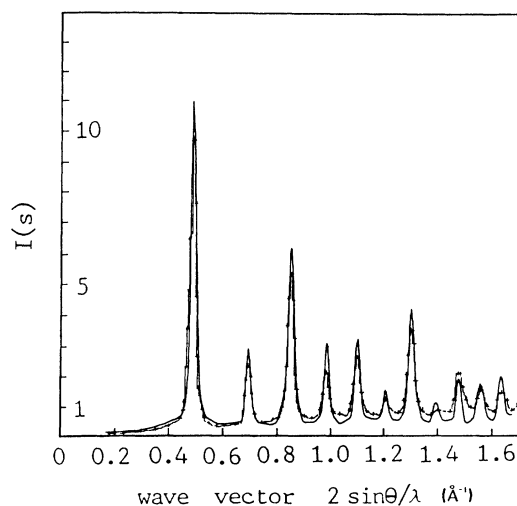


FIG. 9. Comparison of the measured and computed interference functions of nanometer-sized crystalline Fe. To simulate the density deficit, the atoms in the first outer layer are radially moved outwards (expansion) and then randomly displaced the same way as in the case of Fig. 5.

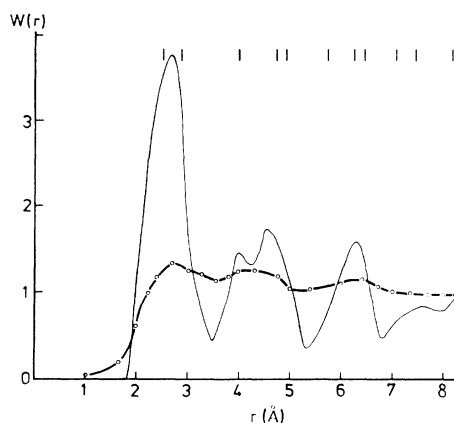


FIG. 10. The computed probability function  $W(r)$  of the grain-boundary component.  $W(r)$  is also called the pair probability function  $g(r)=\rho(r)/\rho_0$ ;  $\rho_0$  is the density of the crystallite.  $W(r)$  [or  $g(r)$ ] was deduced from the computed radial distribution function

$$4\pi r^2 \rho(r) = \frac{1}{N} \sum_{(i \neq j)}^N \sum_{(i \neq j)}^N \delta(r - |\mathbf{r}_i - \mathbf{r}_j|)$$

with the finite-size correction given in Ref. 12, where  $\delta(r)$  is the Dirac delta function, and  $r_i$  and  $N$  are the coordination vector of the  $i$ th atom and the number of the atoms in the grain-boundary component, respectively. (—), grain-boundary component is short-range ordered; -o-, atoms in the grain-boundary component are randomly displaced by 50% and 25% of the NND (as in Fig. 9). The positions of the neighbors in the crystalline (bcc  $\alpha$ -Fe) state are also shown.

sult is shown in Fig. 9. As may be noted from the comparison between Figs. 5 and 9, the density variation and hence the atomic overlapping have little effect on the interference function.

To characterize quantitatively the atomic order in nanometer-sized crystalline materials, the probability function for interatomic distances of the interfacial component was computed for the structural model assuming the grain-boundary component to be short-range ordered (Fig. 4) or to consist of randomly arranged atoms (Figs. 5 and 6). The computed functions are shown in Fig. 10. If the boundary atoms are assumed to exhibit short-range order (Fig. 4), the corresponding probability function shows similar features as a glassy structure. However, if the boundary atoms are displaced by 50% of the NND (Figs. 5 and 6), the corresponding probability function resembles a structure similar to Fig. 1(c), in other words, a structure without short-range order.

### V. SUMMARY

To test the structural model of nanometer-sized crystalline materials, the interference functions of a random ar-

ray of 6-nm bcc Fe crystals were computed by assuming the boundary regions between crystals to be short-range ordered or to consist of randomly displaced atoms. The experimentally observed interference function can only be matched by the computations if the interfacial component of a nanometer-sized crystalline material is assumed to have no short-range order.

### ACKNOWLEDGMENTS

The authors are indebted to Professor Ruppertsberg and his associates (Universitaet des Saarlandes) for valuable advice in performing the x-ray measurements as well as for several very helpful discussions. The previous cooperation with Dr. P. Marquardt (University Cologne) and the discussion with Professor C. N. Wagner, UCLA, are gratefully acknowledged. The work has been financially supported by the Alcoa Foundation, the Bundesministerium für Forschung und Technologie (BMFT, Contract No. 523-4003-03M0023-4), the Deutsche Forschungsgemeinschaft, and the Volkswagen Foundation.

- 
- <sup>1</sup>R. Birringer, U. Herr, and H. Gleiter, *Trans. Jpn. Inst. Met. Suppl.* **27**, 43 (1986). In this reference and others, nanometer-sized crystalline materials have been called nanocrystalline materials.
- <sup>2</sup>H. Gleiter, *Mater. Sci. Eng.* **52**, 91 (1982).
- <sup>3</sup>C. G. Granqvist and R. A. Buhrman, *J. Appl. Phys.* **47**, 2200 (1976).
- <sup>4</sup>C. N. J. Wagner, in *Liquid Metals: Chemistry and Physics*, edited by S. Beer (Dekker, New York, 1972), p. 257.
- <sup>5</sup>D. T. Cromer, *Acta Cryst.* **18**, 17 (1965). D. T. Cromer and J. B. Mann, *Acta Cryst. A* **24**, 321 (1968).
- <sup>6</sup>K. R. Milkove, P. Lamarre, F. Schmueckle, M. D. Vaudin, and

- S. L. Sass, *J. Phys. (Paris)* **46**, C4-71 (1985).
- <sup>7</sup>V. Tiensuu, S. Ergun, and L. Alexander, *J. Appl. Phys.* **35**, 1718 (1964).
- <sup>8</sup>X. Zhu, Ph.D. thesis, Universitaet des Saarlandes, 1986.
- <sup>9</sup>F. Betts and A. Bienenstock, *J. Appl. Phys.* **143**, 4591 (1972).
- <sup>10</sup>E. Nold, P. Lamparter, G. Rainer-Harbach, and S. Steeb, *Z. Naturforsch.* **36a**, 1032 (1981).
- <sup>11</sup>E. Hort, Diploma thesis, Universitaet des Saarlandes, 1986.
- <sup>12</sup>G. S. Cargill III, in *Atomic Energy Review*, edited by U. Gonser (IAEA, Vienna, 1981), Suppl. No. 1.
- <sup>13</sup>J. Harada and K. Ohshima, *Surf. Sci.* **106**, 51 (1981).